Check for updates

JOURNAL OF
CELLULAR
PLASTICS

Original article

Journal of Cellular Plastics
2019, Vol. 55(3) 263–282
© The Author(s) 2019
Article reuse guidelines:
sagepub.com/journals-permissions
DOI: 10.1177/0021955X19839733
journals.sagepub.com/home/cel
SAGE

Thermo-electrical behaviour of cyclic olefin copolymer/exfoliated graphite nanoplatelets nanocomposites foamed through supercritical carbon dioxide

A Dorigato[1], A Biani[1], W Bonani[1,2] and A Pegoretti[1]

Abstract

In this work, novel electrically conductive cyclic olefin copolymer/exfoliated graphite nanoplatelets foams were prepared through a supercritical carbon dioxide treatment starting from the corresponding unfoamed materials prepared by melt compounding, in order to investigate their thermo-electrical properties. For both unfoamed and foamed samples, the exfoliated graphite nanoplatelets introduction led to a systematic enhancement of the thermal degradation temperature. Dynamic-mechanical thermal analysis revealed that the nanofiller addition promoted an enhancement of the storage modulus and of the glass transition temperature over the whole range of the applied foaming pressures. While for unfoamed materials exfoliated graphite nanoplatelets introduction determined an important decrease of the electrical resistivity, the foaming process induced the breakage of the conductive path, with a consequent increase of electrical resistivity. Evaluation of the surface heating upon voltage application showed that the surface temperature of unfoamed materials could be noticeably increased at relatively low voltage levels, while a less pronounced surface heating could be obtained with the corresponding nanocomposite foams.

[1]Department of Industrial Engineering and INSTM Research Unit, University of Trento, Trento, Italy
[2]Department of Industrial Engineering and BIOtech Research Centre, University of Trento, Trento, Italy

Corresponding authors:
A Dorigato and A Pegoretti, Department of Industrial Engineering and INSTM Research Unit, University of Trento, Via Sommarive 9, 38123 Trento, Italy.
Emails: andrea.dorigato@unitn.it; alessandro.pegoretti@unitn.it

Keywords
Cyclo olefin copolymer, supercritical carbon dioxide, nanocomposites, foams, dynamical mechanical analysis, electrical properties

Introduction

A particular interest has been recently devoted to cyclic olefin copolymers (COCs),[1,2] an innovative class of amorphous thermoplastics obtained by copolymerization of norbornene and ethylene through metallocene-based catalysis.[3] Being characterized by elevated stiffness, high chemical resistance, low density and good barrier properties, these materials are interesting from a technological point of view. COCs grades with different glass transition temperature (T_g) are now available in the market.[4–6] In particular, COCs are applied in the production of transparent injection moulding parts such as food containers, drug blisters, medical and diagnostic devices. Currently, COCs utilization in electronic packaging field is very limited due to their intrinsic low electrical conductivity. In fact, it is well known that static electricity can be transferred to the surface of insulating materials, leading to an electrostatic discharge that can seriously damage electrical devices. Electrostatic discharge (ESD) materials are a new class of plastics that reduce the backlog of static electricity to protect electrostatic-sensitive devices. In these products, a good electrical conductivity of the material prevents electrostatic discharge phenomena, ensuring safe storage and functional integrity of electronic devices. In addition, the possibility to electrically heat COCs food and drug containers in order to perform thermal sterilization and/or pasteurization upon voltage application could represent a stimulating technological advancement of the packaging field. In this respect, COCs compounding with electrically conductive nanostructured fillers could represent an effective opportunity to prepare electroactive polymeric materials.

Nanocomposites represent an innovative class of multifunctional materials in which the additivation of nanofillers at limited concentrations (5–10 wt%) within a polymer matrix can effectively enhance the mechanical, thermal and electrical properties with respect to the pristine matrix.[7] In the recent years, particular attention has been devoted in the open literature to nanocomposite systems filled with conductive nanofillers such as graphene and carbon nanotubes,[8–10] but also with carbonaceous plate-like nanofillers such as exfoliated graphite nanoplatelets (xGnP).[11–17] This nanofiller is constituted by very thin crystalline graphite lamellae, stacked in several layers of crystalline graphite. Because of the honeycomb arrangement of the carbon atoms within the crystal lattice, xGnP possesses outstanding stiffness, strength[18] and electrical conductivity values. For these peculiar properties, a homogeneous distribution of this nanofiller within a polymer matrix[19,20] allows to produce polymer composites with superior electromechanical properties of polymer composites.[11,12]

Considering the possible applications of COCs in the electronic packaging field, a weight reduction through the matrix foaming process is a desirable process. Moreover, a reduction of the material density can determine several advantages in terms of fuel saving in transportations and important natural resources savings. From a technological point of view, polymeric foams are generally applied in automotive, aerospace, construction and in packaging field[21] and also for the insulation of building constructions.[22]

Traditional production processes of the porous plastics are based on the physical blowing by low boiling hydrocarbons or their halogenated derivatives. Therefore, about 15 billion kilograms of these solvents are produced worldwide every year, with heavy environmental problems related to the emission of toxic compounds and of polluted waste water production.[23] For these reasons, traditional blowing agents (i.e. pentane, butane, chlorofluoro hydrocarbons) have been recently withdrawn and replaced by eco-friendly gases (i.e. argon, nitrogen and carbon dioxide).[24] In this sense, an interesting technological possibility is represented by the application of supercritical fluids (SFCs) to produce polymer foams.[25–34] SCFs possess intermediate physical properties among gases and fluids, with a density and a diffusion coefficient similar to that of the liquids and a viscosity comparable to that of the gases.[35] Polymer matrix foaming with supercritical fluids allows avoiding organic solvents and presents several advantages from a chemical, physical and toxicological point of view. Moreover, it can be successfully applied also on industrial scale. Because of its easy processability, cheapness, non-toxicity and non-flammability,[36,37] carbon dioxide is the most utilized supercritical fluid.

In the literature, it is possible to find some works on the mechanical behaviour of xGnP-based nanocomposites foamed through supercritical carbon dioxide ($scCO_2$),[38–40] but only marginal attention has been devoted to their thermo-electrical behaviour.[41,42] Moreover, only few papers dealing with the physical properties of COC/xGnP (or graphene) foamed through $scCO_2$ can be found in literature.[43–45] In a previous paper of our group, a COC matrix was compounded with xGnP at different concentrations, and the resulting nanocomposites were foamed at various pressures by $scCO_2$.[46] It was shown that the density of the obtained foams decreased with the foaming pressure, and xGnP introduction limited the cell growth during the expansion process, thus reducing the cell diameter. These morphological features, combined with the exfoliation and orientation of the nanoplatelets along the cell walls, determined noticeable improvements of the modulus and of the creep stability.

On the basis of these considerations and of the results presented in our papers on COC nanocomposite foams,[46,47] the objective of the present work is to prepare and characterize COC/xGnP systems at various filler loadings, to be then foamed through a $scCO_2$ process. A general comparison between unfoamed and foamed samples will be then carried out, in order to evaluate the real effectiveness of xGnP nanoparticles in improving the thermo-mechanical properties and the electrical behaviour of the resulting foams.

Experimental part

Materials

Polymeric granules of a Topas 8007 COC (melt flow index at 2.16 kg, 190°C = 2.17 g/10min, density = 1020 kg/m^3), supplied by Ticona (Florence, Kentucky, USA), were utilized as matrix. Exfoliated graphite nanoplatelets xGnP-M-5 (specific surface area of 120 m^2/g, mean diameter of 5 μm and thickness of 6–8 nm[16]) were provided by XG Sciences Inc. (East Lansing, Michigan, USA). Both materials were used as received.

Samples preparation

Unfoamed samples preparation. As previously reported,[46,47] the xGnP filler was melt compounded with COC in a Thermo Haake internal mixer at a temperature of 190°C and a rotor speed of 90 rpm. In order to prevent nanoparticles agglomeration and to promote a complete and homogeneous mixing, a compounding time of 15 min was utilized. The compounded materials were then hot pressed at 0.002 bar for 10 min at a temperature of 190°C in a Carver press, to prepare 0.8 mm thick square sheets. In this study, COC/xGnP unfoamed nanocomposites were developed at different concentrations (1 wt%, 2 wt%, 5 wt% and 10 wt%). Unfoamed materials were designated indicating the matrix, the nanofiller type and loading. As an example, COC-xGnP-1 denotes the nanocomposite unfoamed sample with an xGnP content of 1 wt%.

Foaming process. As reported in our previous papers on COC nanocomposites foams,[46,47] foamed samples were prepared through a scCO_2 treatment. The carbon dioxide in liquid/vapour equilibrium state was supplied by Messer Italia S.r.l. (Padova, Italy) with a gas purity greater than 99.5 vol% in a pressure vessel (60 bar at room temperature). Foamed samples were prepared starting from solid rectangular specimens: 0.5 cm wide and 2 cm long. Neat COC copolymer and relative COC/xGnP unfoamed nanocomposites were placed in a stainless steel 316Ti reaction chamber (BR-300, Berghof Products + Instruments, Eningen, Germany) with an internal polytetrafluoroethylene liner. A reaction vessel having a capacity of 700 ml, a diameter of 60 mm and a height of 250 mm, with a maximum pressure of 200 bar and a temperature of 260°C, was utilized. The reactor cap was equipped with fluid inlet valve, pressure relief valve and safety valve, a submersion thermocouple and a pressure sensor connected to a computer. In order to cool the CO_2 lines and pump head, a cryostatic bath with a temperature of −9°C (Model M408-BC, MPM Instruments s.r.l., Bernareggio, MB, Italy) was utilized. Once the system had been sealed, liquid CO_2 was pumped into the reactor and pressurized till the supercritical conditions were reached through a high-performance liquid chromatographic pump (Model 426, Alltech, Deerfield, IL, USA). The temperature of the reactor was controlled through an electrical heating jacket (BHM 700, Berghof) run by a BDL-3000 temperature controller (Berghof). In this way, neat COC and nanocomposite

samples foamed with $scCO_2$ at four different pressures (90, 110, 130 and 150 bar) for 30 min were prepared. A reaction temperature of 95°C (i.e. 15°C higher than COC glass transition temperature) was maintained. Foaming was obtained upon fast depressurization from supercritical to room conditions. A detailed description of the experimental equipment of the foaming process and of the experimental conditions at which the prepared materials were subjected during the foaming process can be found in our previous paper on COC nanocomposite foams.[46] Foamed samples were denoted indicating the matrix, the filler type, the filler content and the foaming pressure. As an example, COC-xGnP-5_e90 indicates nanocomposite foam with a filler amount of 5 wt%, expanded with depressurization from 90 bar. Table 1 summarizes the list of the prepared samples.

Experimental methodologies

Thermo-mechanical properties. TGA was performed trough a Mettler TG50 thermobalance by using an ambient air flow of 150 ml/min. Samples were tested from 50°C to 700°C at a heating rate of 10°C/min. Both unfoamed and foamed materials were considered. The decomposition temperature (T_d), corresponding to the temperature associated to the maximum mass loss rate, was evaluated.

Dynamic-mechanical thermal analysis (DMTA) was conducted through a Q800 DMA machine (TA Instruments, USA). Rectangular samples 5 mm wide and 1 mm thick were tested at a frequency of 1 Hz (gage length of 10 mm) in a temperature interval between 20°C and 120°C at a heating rate of 3°C/min. The temperature dependency of the storage modulus (E') and of the loss tangent ($\tan\delta$) was therefore determined. The glass transition temperature (T_g), i.e. the temperature corresponding to the $\tan\delta$ peak, was evaluated.

Electrical properties. The electrical resistivity of unfoamed and foamed materials was measured according to D4496-13 standard through a Keithley model 6517A multimeter (Keithley Instrument, Inc., Cleveland, OH, USA), in a four-point configuration. Both unfoamed samples and materials foamed at 150 bar were considered. As specified by the standard, the applied voltage was kept constant for all the specimens at a value of 10 V, in order to maintain the power input lower than 1 W. The resistivity value was determined as reported in equation (1)

$$\rho = R \cdot \frac{A}{t} \tag{1}$$

where R is the volume resistance (expressed in Ω), A is the cross area of the specimen (cm^2) and t is the distance between the two inner probes where the voltage is measured (cm).

In order to evaluate the surface heating upon voltage application through the Joule effect, a Ti9 Thermal Imagers FLUKE® infrared (IR) thermographic camera was used. COC-xGnP-15, COC-xGnP-20 and COC-xGnP-20_e150 samples were

Table 1. List of the prepared samples.

Sample code	xGnP loading (wt%)	foaming pressure (bar)
COC	–	–
COC-xGnP-1	1	–
COC-xGnP-2	2	–
COC-xGnP-5	5	–
COC-xGnP-10	10	–
COC-xGnP-15	15	–
COC-xGnP-20	20	–
COC_e90	–	90
COC-xGnP-1_e90	1	90
COC-xGnP-2_e90	2	90
COC-xGnP-5_e90	5	90
COC-xGnP-10_e90	10	90
COC_e110	–	110
COC-xGnP-1_e110	1	110
COC-xGnP-2_e110	2	110
COC-xGnP-5_e110	5	110
COC-xGnP-10_e110	10	110
COC_e130	–	130
COC-xGnP-1_e130	1	130
COC-xGnP-2_e130	2	130
COC-xGnP-5_e130	5	130
COC-xGnP-10_e130	10	130
COC_e150	–	150
COC-xGnP-1_e150	1	150
COC-xGnP-2_e150	2	150
COC-xGnP-5_e150	5	150
COC-xGnP-10_e150	10	150
COC-xGnP-15_e150	15	150
COC-xGnP-20_e150	20	150

COC: cyclic olefin copolymer; xGNP: exfoliated graphite nanoplatelets.

tested at different voltages for 300 s. The evolution of the surface temperature as a function of time was measured. The list of the applied voltages for each sample is reported in Table 2.

Results and discussion

Thermo-mechanical behaviour

Considering a possible application of the prepared samples as electro-active nanocomposite materials that can be heated through Joule effect, an important feature

Table 2. Voltage levels applied for the evaluation of the surface heating.

Sample	Applied voltage (V)
COC-xGnP-15	20, 50, 100, 120, 150, 190, 220
COC-xGnP-20	20, 50, 100, 120, 150
COC-xGnP-20_e150	50, 100, 220

COC: cyclic olefin copolymer; xGNP: exfoliated graphite nanoplatelets.

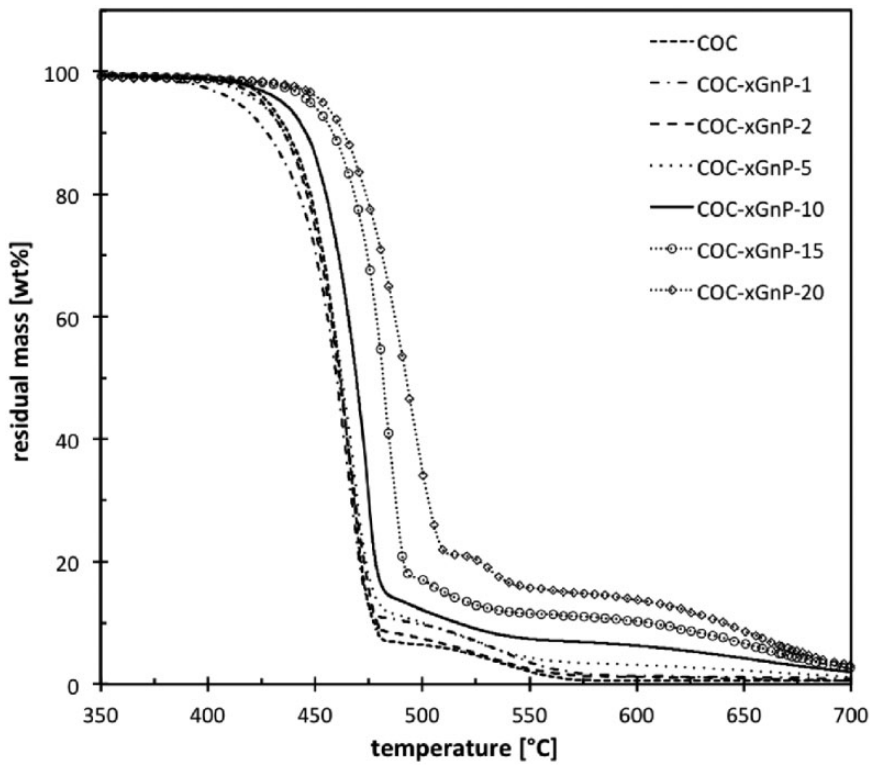

Figure 1. TGA thermograms of neat COC and relative unfoamed nanocomposites samples. COC: cyclic olefin copolymer; xGNP: exfoliated graphite nanoplatelets.

that must be investigated is thermal stability against thermo-oxidative degradation. For this reason, thermogravimetric analysis (TGA) was performed under air flow. The TGA thermograms presented in Figure 1 report the weight loss as a function of the temperature for unfoamed materials. A sharp mass drop associated with the thermal degradation of the polymer matrix can be detected above 450°C. Moreover, the residual mass at 700°C is virtually equal to zero for neat COC, while

Table 3. Thermal degradation temperature (T_d) from TGA tests on neat COC and relative unfoamed nanocomposites.

Sample	T_d (°C)
COC	466.1
COC-xGnP-1	465.0
COC-xGnP-2	465.4
COC-xGnP-5	468.1
COC-xGnP-10	473.5
COC-xGnP-15	484.2
COC-xGnP-20	494.1

COC: cyclic olefin copolymer; xGNP: exfoliated graphite nanoplatelets.

a mass residue proportional to the nanofiller content can be observed for the nanocomposites. As reported in literature, this mass residue is due to an incomplete combustion of the material, promoted by the matrix charring in the nanofilled samples.[48] The prepared nanocomposites showed an increment of the thermal degradation temperature (T_d) values proportionally to the xGnP amount (Table 3). The T_d values of COC-xGnP-1 and COC-xGnP-2 samples are practically the same of the neat COC matrix (466°C), while the improving effect due to xGnP introduction, even if not so pronounced, starts to be evident for nanofiller contents higher than 5 wt%. For instance, with an xGnP content of 20 wt%, a T_d increment of 20°C can be observed. Therefore, TGA tests highlighted how the thermal stability of the nanocomposite samples is noticeably enhanced with respect to the neat matrix. Similar results were previously observed by our group on COC samples filled with silica nanoparticles.[49] In Figure 2(a), representative TGA curves of the materials foamed at a pressure of 130 bar with different nanofiller loadings are reported, while Figure 2(b) shows the corresponding T_d values. The increment in the thermal degradation temperature upon xGnP addition is clear over the whole range of the applied pressures. On the other hand, the dependency of T_d values from the applied pressure cannot be clearly identified. Considering that the differences between the samples foamed at different pressure with the same xGnP amount are not so high (less than 7°C–8°C), it can be concluded that the foaming pressure does not substantially affect the degradation temperature of the materials, if materials with the same xGnP amount are compared. The obtained results are in agreement with some studies present in literature. In fact, Gedler et al. reported that well-dispersed graphite nanoplatelets improved the thermal stability of polycarbonate foams due to their barrier effect, delaying the diffusion of volatile products during the degradation process. For the degradation in air, the graphene nanoplatelets created a tortuous path for air, delaying the thermo-oxidative degradation of the material.[39]

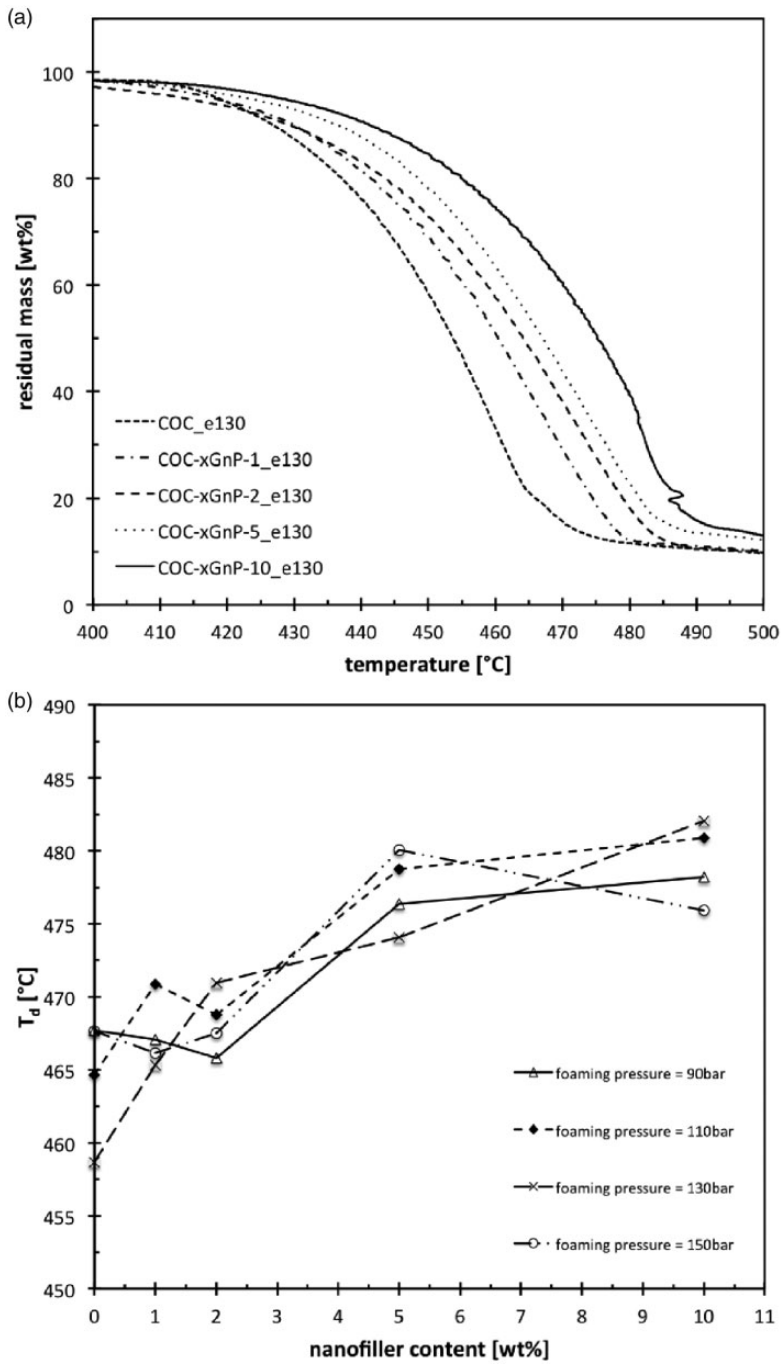

Figure 2. (a) TGA thermograms of neat COC and relative nanocomposite materials foamed at 130 bar. (b) T_d values of the neat COC and relative nanocomposite materials foamed at different foaming pressures. T_d: thermal degradation temperature; COC: cyclic olefin copolymer; xGNP: exfoliated graphite nanoplatelets.

It is also important to evaluate the mechanical stability of the prepared materials as a function of the service temperature. Therefore, it could be useful to evaluate the effect of the xGnP addition on the viscoelastic properties of unfoamed and foamed samples through DMTA tests. In Figure 3(a) and (b), the storage modulus (E′) and the loss tangent (tanδ) curves of unfoamed samples are, respectively, reported. The storage modulus shows a remarkable enhancement with increasing the nanofiller content, while the loss tangent values are inversely proportional to the xGnP amount. For instance, an interesting increase in the E'_{20} of about 28% with respect to the neat COC can be obtained by adding 10 wt% of xGnP, while with 20 wt% of xGnP, the observed increment is even more pronounced (about 65%). These results demonstrate the effectiveness of xGnP in increasing the stiffness of the materials. The increase of the material rigidity was already observed under quasi-static conditions in our previous work focused on the mechanical behaviour of COC/xGnP nanocomposites.[46] Also, the glass transition temperature seems to be strongly affected by the xGnP addition, in fact the loss tangent peak of the unfoamed samples is shifted at higher temperatures. From Table 4, the E'_{20} and the T_g values as a function of the xGnP content are reported. The T_g is observed to increase of about 7°C with a nanofiller amount of 20 wt%. As reported in some works, the glass transition increment obtained by adding graphitic nanofillers can be explained by the restricted mobility of the amorphous fraction of polymer macromolecules[50,51] within the polymer matrix. In Figure 4(a) and (b), representative curves of the storage modulus and loss tangent curves for the materials expanded at 130 bar with different nanofiller contents are, respectively, reported. In Figure 4(c), the E'_{20} values of the foamed materials as a function of the xGnP loading are shown. It can be noticed that E'_{20} still increases with the nanofiller content in the whole range of applied pressures but in a more pronounced way with respect to the corresponding unfoamed materials. For instance, an E'_{20} increment of about 3.5 times with respect to the neat matrix can be observed by adding 10 wt % of nanofiller at a foaming pressure of 130 bar. As it could be expected, the E'_{20} decreases with the applied pressure because of a more intense foaming. The increase in the stiffness of the prepared foams due to the xGnP addition was already observed in our previous work on the mechanical behaviour of COC/xGnP nanocomposites foams.[46] In that paper, it was clarified that the enhancement of the foam stiffness was partially both due to a change in the foams density and to the addition of xGnP. A systematic increase of density with the nanofiller amount was observed over the whole range of applied pressures (from 8 cells/mm^3 up to 61 cells/mm^3 with an xGnP amount of 10wt% at an applied pressure of 90 bar). Considering the density variation due to nanofiller addition in unfoamed samples, it was clear that the density increase in the nanocomposite foams could not be simply explained by the higher density of xGnP but also by a morphological change within the foam microstructure (i.e. cell density and cell size). In fact, as the foaming pressure increased, a systematic density reduction was observed for all the compositions (from 61 cells/mm^3 to 45 cells/mm^3 for the 10 wt% nanocomposite foam, passing from 90 bar up to 150 bar). This could be due to the fact that at

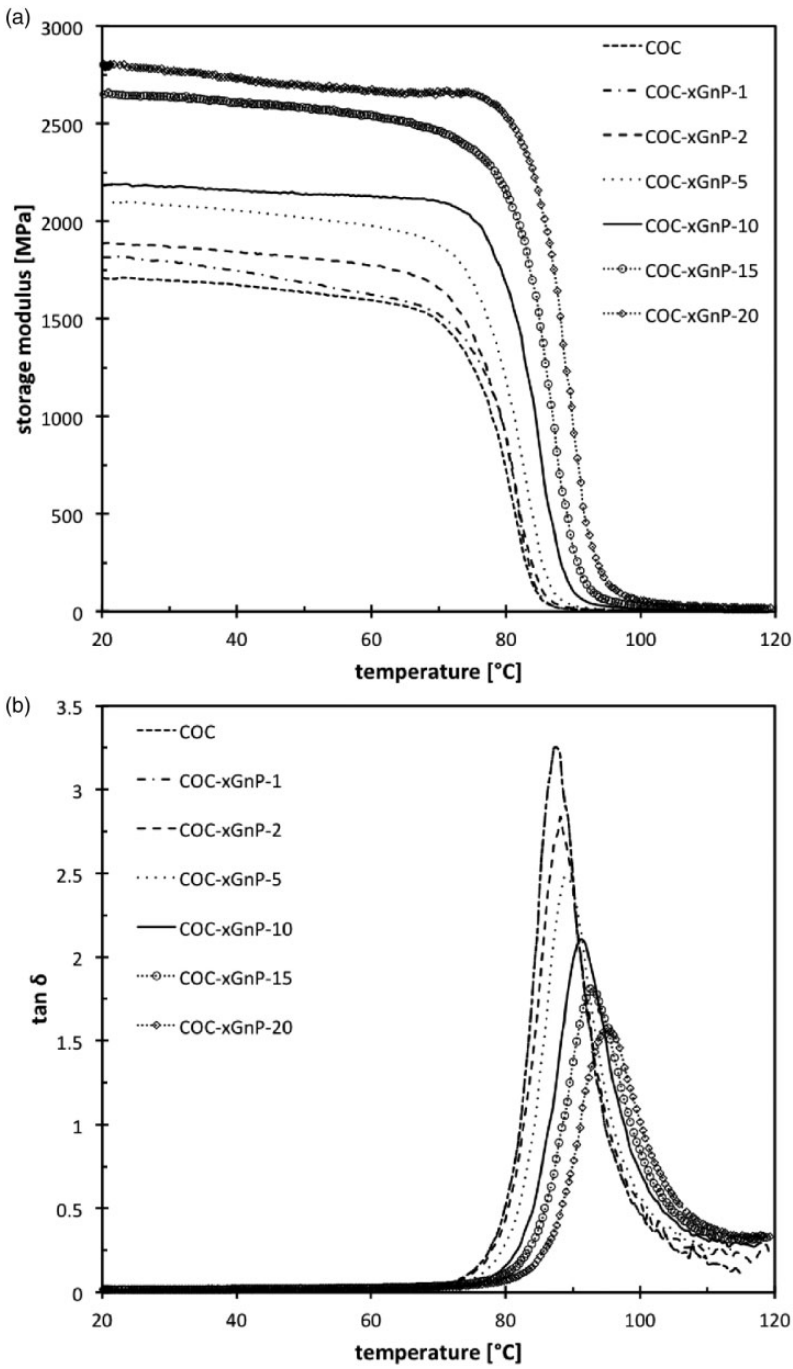

Figure 3. DMTA on neat COC and relative unfoamed nanocomposites. (a) Storage modulus (E′) and (b) loss tangent curves (tanδ) as a function of the testing temperature. COC: cyclic olefin copolymer; xGNP: exfoliated graphite nanoplatelets.

Table 4. Storage modulus evaluated at 20°C (E'_{20}) and the glass transition temperature (T_g) from DMTA tests on neat COC and relative unfoamed nanocomposites.

Sample	E'_{20} (MPa)	T_g (°C)
COC	1707	87.6
COC-xGnP-1	1816	87.6
COC-xGnP-2	1887	88.1
COC-xGnP-5	2097	88.7
COC-xGnP-10	2183	91.3
COC-xGnP-15	2652	92.5
COC-xGnP-20	2808	94.5

COC: cyclic olefin copolymer; xGNP: exfoliated graphite nanoplatelets; DMTA: dynamic-mechanical thermal analysis.

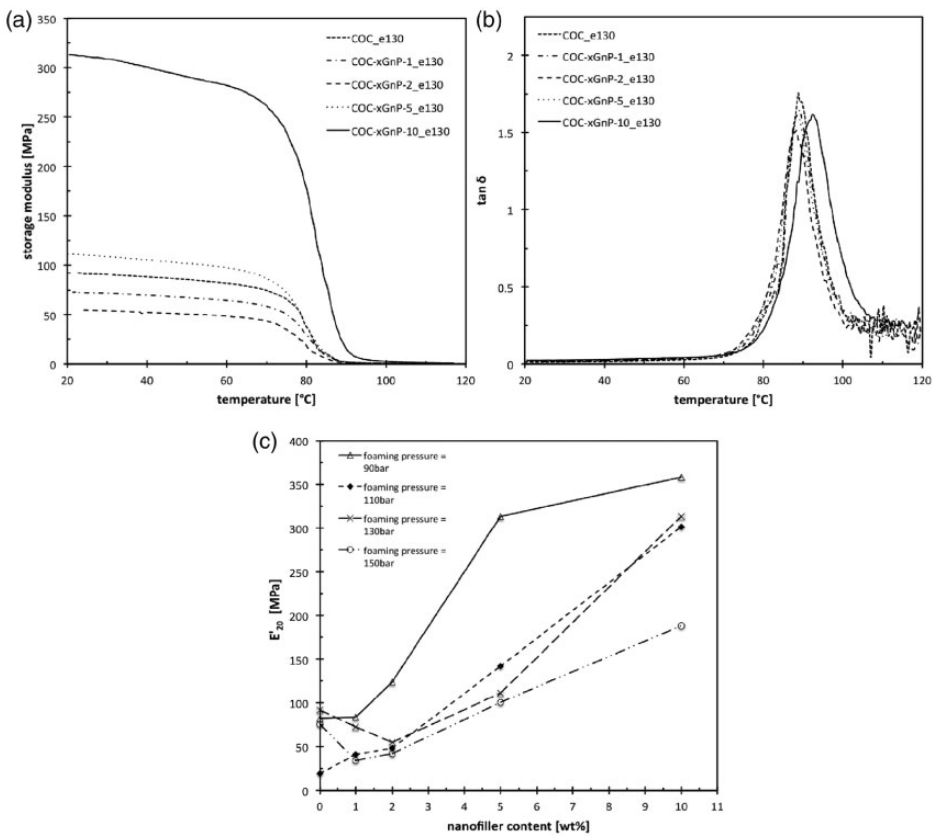

Figure 4. DMTA tests on neat COC and relative nanocomposites foamed at 130 bar. (a) Storage modulus (E′), (b) loss tangent (tanδ). (c) Storage modulus evaluated at 20°C (E'_{20}) as a function of the nanofiller content for different foaming pressures. COC: cyclic olefin copolymer; xGNP: exfoliated graphite nanoplatelets.

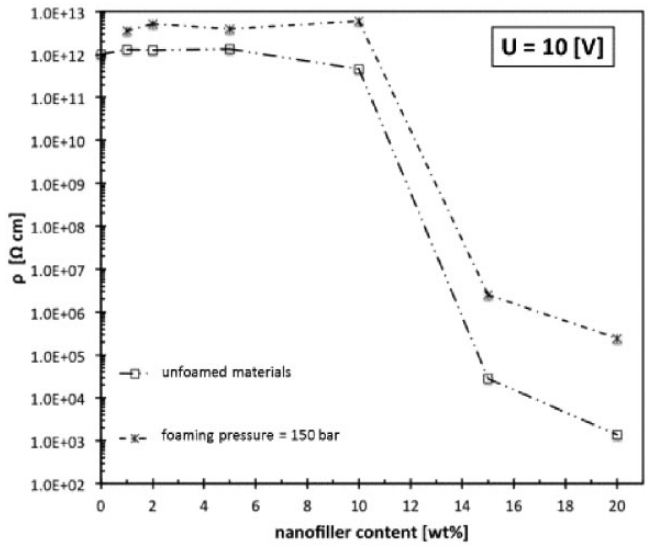

Figure 5. Electrical resistivity on neat COC and relative nanocomposites for unfoamed and foamed materials at a pressure of 150 bar (applied voltage equal to 10 V).

elevated pressures, the diffusion of the $scCO_2$ within the matrix was favoured and the foaming process was more efficient. On the other hand, morphological observation through field emission scanning electron microscopic (FESEM) analysis highlighted that the occurrence of xGnP exfoliation and orientation along the cell wall given by the foaming pressure could increase the mechanical properties of the matrix itself and therefore the stiffness of the resulting foams. Also for the foamed materials, xGnP addition leads to a sensible enhancement of the glass transition temperature (about 3°C with 10 wt% of nanofiller). Considering that for an amorphous matrix, the glass transition temperature is generally considered as the maximum service temperature, the observed T_g enhancement due to nanofiller addition can be important to extend the application range of these materials.

Electrical behaviour

Considering the possible application of these nanocomposites as ESD materials or for the electroactive packaging, it is important to evaluate their electrical behaviour. In Figure 5, the electrical resistivity values as a function of the nanofiller content for unfoamed materials and nanocomposite foams are reported. A strong decrease of the electrical resistivity can be detected for nanofiller amounts higher than 10 wt%, both for the unfoamed and for the foamed materials. In particular, with a nanofiller loading of 20 wt%, an electrical resistivity of 1.4×10^3 Ω·cm and of 2.44×10^5 Ω·cm can be obtained for unfoamed samples and materials foamed at 150 bar, respectively. As reported in our previous paper on electrical behaviour of

nanocomposite materials,[15] after a critical filler amount (i.e. the percolation threshold), lateral connection between xGnP nanoplatelets is formed, making possible the conduction of the electrical current within the material. Similar results were reported in literature in the studies on the electrical characterization of Poly (methyl methacrylate) (PMMA)/functionalized graphene oxide nanocomposites[52] and COC/expanded graphite unfoamed nanocomposites.[53]

It should be noted that the electrical resistivity of the foamed materials at 150 bar is systematically higher than that of the corresponding unfoamed samples, even if the percolation threshold remains the same (i.e. 10 wt%). This fact can be due to the porous structure of the foam. In these conditions, the effective cross area of the tested samples is strongly reduced. It also has to be taken into account the effect of the foaming process on the microstructural features of the materials. In our previous work on COC/xGnP nanocomposite foams, FESEM images highlighted an evident alignment of the xGnP nanoplatelets along the cellular wall, especially at elevated foaming pressures.[46] In these conditions, the formation of a percolative network due to the contact between the nanoplatelets is hindered by the matrix foaming, especially at elevated pressures, when the nanofiller alignment is more pronounced. In the foamed materials, the formation of the conductive path is possible only when the lateral contacts between xGnP nanoplatelets are formed (i.e. at elevated filler amounts). The same considerations have been reported in our previous work on electrically conductive polyamide 12 nanocomposites for industrial applications.[54] In that paper, it was shown that carbonaceous nanofiller oriented itself along the extrusion/drawing direction, and only at higher filler contents, nanofiller aggregates started contacting each other forming a conductive network within the polymer, thus decreasing the electrical resistivity. Another microstructural aspect that can be considered to explain the obtained results was reported by Xu et al.[55] in their work on conductive multi-walled carbon nanotubes/polyurethane nanocomposite foams, where they showed that nanofiller preferentially localized in the cell-struts (the interconnecting point of the surrounding bubbles). Consequently, an increase in the pore size results in an increase of the distance between adjacent struts, hence promoting the breakage of the conductive network. It can be therefore concluded that matrix foaming seems to negatively affect the electrical conductivity of the investigated nanocomposites.

It is now important to evaluate the surface heating capability of the prepared materials upon voltage application (i.e. through Joule effect). In order to obtain a significant surface heating effect, only nanocomposite materials at elevated filler loading were considered. In Figure 6(a), images of the COC-xGnP-20 sample taken by the thermographic camera with an applied voltage of 120 V are reported, while in Figure 6(b), the evolution of the surface temperature at different voltage levels is reported. From Figure 6(a), it is evident that the increase of the temperature within the material upon a voltage application is substantially homogenous, and only near the sample edges, a lower temperature can be observed. From Figure 6(b), it is clear that an appreciable heating can be obtained even at limited voltage levels.

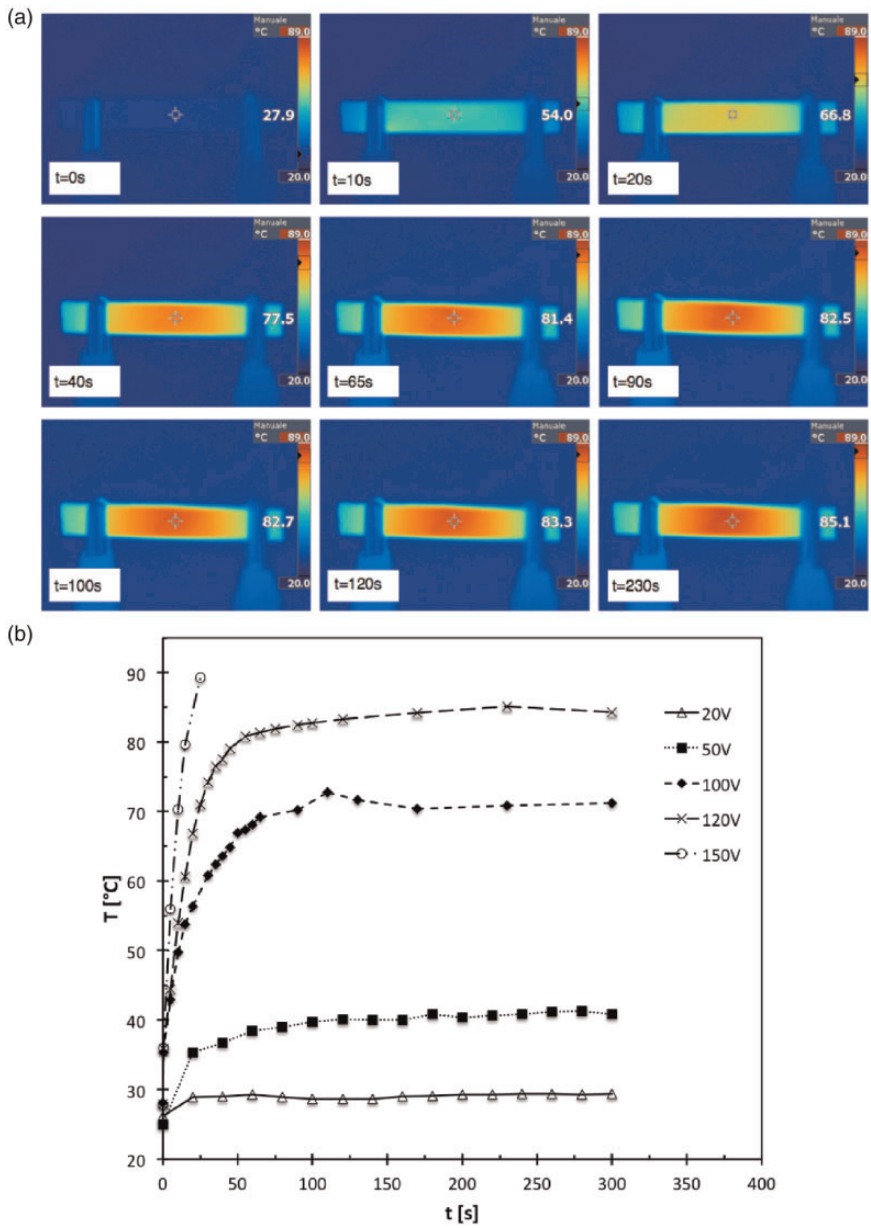

Figure 6. (a) IR thermocamera images of the surface temperature evolution for COC-xGnP-20 sample (applied voltage of 120 V). (b) Evaluation of the surface temperature of COC-xGnP-20 sample at different applied voltages.

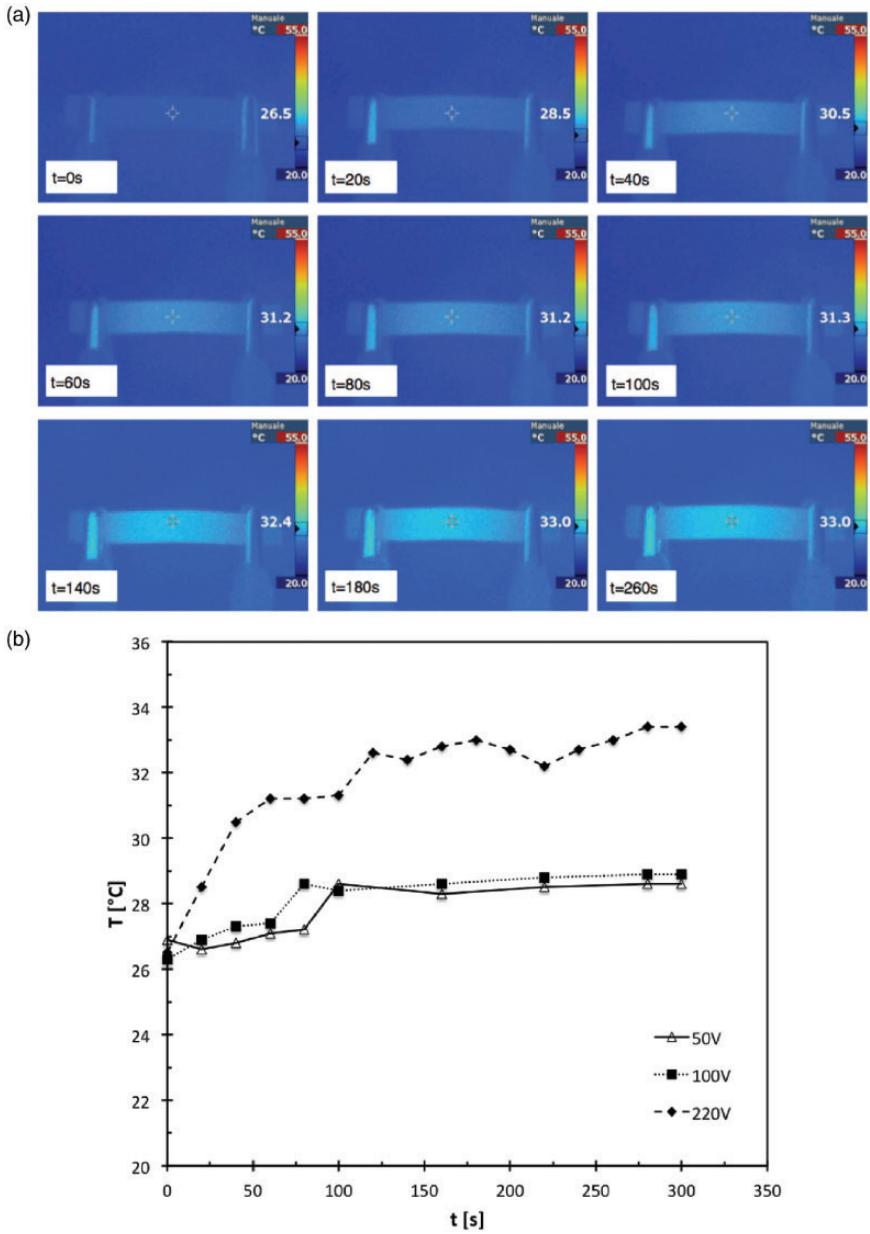

Figure 7. (a) IR thermocamera images of the surface temperature evolution for COC-xGnP-20_e150 sample (applied voltage of 220 V). (b) Evaluation of the surface temperature with time of COC-xGnP-20_e150 sample at different applied voltages.

In fact, with an applied voltage of 50 V, the surface temperature is 40°C after 70 s, while at 120 V, a temperature greater than 80°C can be reached in the same time. While at 150 V a rapid increase of the surface temperature can be observed, for voltage levels lower than 150 V a stabilization of the surface temperature can be detected, even after 300 s. This means that the sample reached a thermal equilibrium, because the heat flow produced through the Joule effect is equal to the dissipated thermal power. This temperature plateau could be important for the preparation of electro-active devices in which the thermal degradation for prolonged application of the electrical stimulus should be avoided. The surface heating upon voltage application was investigated also in the foamed material. In Figure 7(a), images of the COC-xGnP-20_e150 sample taken by the IR thermographic camera with an applied voltage of 220 V are reported, while in Figure 7 (b), the evolution of the surface temperature at different applied voltages is reported. Even in this case, a homogeneous distribution of the surface temperature within the sample can be observed, but a very limited temperature increase can be obtained with an applied voltage of 220 V (7°C increase after 200 s). This result can be explained considering the higher electrical resistivity value reported for the foamed materials (see Figure 5). Therefore, electrical heating of nanocomposite foams is less effective than that observed for the corresponding unfoamed materials, and further efforts will be required to obtain a satisfactory heating of the nanocomposite foams through Joule effect.

Conclusions

The thermoelectrical behaviour of COC/xGnP nanocomposites, prepared through melt compounding and foamed through a $scCO_2$ process, was investigated, in order to assess their applicability as electroactive packaging materials. It was found that the introduction of xGnP into the neat COC resulted in significant improvements of the thermal degradation temperature, both for unfoamed samples and for the foamed materials. DMTA showed a noticeable enhancement of the storage modulus and of the glass transition temperature with the xGnP amount. Nanofiller introduction led to an important volume resistivity decrease of unfoamed materials up to 10^3 Ω·cm for xGnP loadings higher than 10 wt%. The foamed materials showed a systematic increase of the volume resistivity with respect to the corresponding unfoamed samples. Evaluation of the surface temperature upon voltage application demonstrated how it is possible to obtain a rapid heating of the unfoamed samples at relatively low voltage levels, while the lower conductivity of the foams leads to a limited surface temperature increase.

Declaration of conflicting interests

The author(s) declared no potential conflicts of interest with respect to the research, authorship, and/or publication of this article.

Funding

The author(s) received no financial support for the research, authorship, and/or publication of this article.

References

1. Ou CF and Hsu MC. Preparation and properties of cycloolefin copolymer/silica hybrids. *J Appl Polym Sci* 2007; 104: 2542–2548.
2. Ou CF and Hsu MC. Preparation and characterization of cyclo olefin copolymer (COC)/silica nanoparticle composites by solution blending. *J Polym Res* 2007; 14: 373–378.
3. Arndt M and Beulich I. C1-symmetric metallocenes for olefin polymerisation, 1. Catalytic performance of [Me2C (3-tertBuCp)(Flu)] ZrCl2 in ethene/norbornene copolymerisation. *Macromol Chem Phys* 1998; 199: 1221–1232.
4. Forsyth JF, Scrivani T, Benavente R, et al. Thermal and dynamic mechanical behavior of ethylene/norbornene copolymers with medium norbornene contents. *J Appl Polym Sci* 2001; 82: 2159–2165.
5. Kolařík J, Pegoretti A, Fambri L, et al. High-density polyethylene/cycloolefin copolymer blends, part 2: nonlinear tensile creep. *Polym Eng Sci* 2006; 46: 1363–1373.
6. Mandalia T and Bergaya F. Organo clay mineral–melted polyolefin nanocomposites effect of surfactant/CEC ratio. *Journal of Physics and Chemistry of Solids* 2006; 67: 836–845.
7. Ajayan PM, Schadler LS and Braun PV. *Nanocomposite science and technology*. Hoboken: John Wiley & Sons; 2006.
8. Han Z and Fina A. Thermal conductivity of carbon nanotubes and their polymer nanocomposites: a review. *Prog Polym Sci* 2011; 36: 914–944.
9. Singh V, Joung D, Zhai L, et al. Graphene based materials: past, present and future. *Prog Mater Sci* 2011; 56: 1178–1271.
10. Stankovich S, Dikin DA, Dommett GH, et al. Graphene-based composite materials. *Nature* 2006; 442: 282–286.
11. Drzal LT and Fukushima H. Exfoliated graphite nanoplatelets (xGnP): a carbon nanotube alternative. *Proc NSTI Nanotechnol Conf Trade Show* 2006; 1: 170–173.
12. Kalaitzidou K, Fukushima H and Drzal LT. Mechanical properties and morphological characterization of exfoliated graphite–polypropylene nanocomposites. *Compos A Appl Sci Manuf* 2007; 38: 1675–1682.
13. Kim S, Do I and Drzal LT. Thermal stability and dynamic mechanical behavior of exfoliated graphite nanoplatelets – LLDPE nanocomposites. *Polym Compos* 2010; 31: 755–761.
14. Park HM, Kalaitzidou K, Fukushima H, et al. *Exfoliated graphite nanoplatelet (xGnP)/polypropylene nanocomposites*. East Lansing: Michigan State University, Composite Materials & Structures Center, 2007.
15. Pedrazzoli D, Dorigato A and Pegoretti A. Monitoring the mechanical behaviour of electrically conductive polymer nanocomposites under ramp and creep conditions. *J Nanosci Nanotech* 2012; 12: 4093–4102.
16. Pedrazzoli D, Dorigato A and Pegoretti A. Monitoring the mechanical behaviour under ramp and creep conditions of electrically conductive polymer composites. *Composites A* 2012; 43: 1285–1292.

17. Persson H, Yao Y, Klement U, et al. A simple way of improving graphite nanoplatelets (GNP) for their incorporation into a polymer matrix. *Express Polym Lett* 2012; 6: 142–147.
18. Pierson HO. *Handbook of carbon, graphite, diamonds and fullerenes: processing, properties and applications*. Norwich: William Andrew, 2012.
19. Liu WW, Chai S-P, Mohamed AR, et al. Synthesis and characterization of graphene and carbon nanotubes: a review on the past and recent developments. *Journal of Industrial and Engineering Chemistry*. 2014; 20: 1171–1185.
20. Mittal G, Dhand V, Rhee KY, et al. A review on carbon nanotubes and graphene as fillers in reinforced polymer nanocomposites. *J Indus Eng Chem* 2015; 21: 11–25.
21. Kozlowski M. *Lightweight plastic materials*. London: INTECH Open Access Publisher, 2012.
22. Papadopoulos AM. State of the art in thermal insulation materials and aims for future developments. *Energy Build* 2005; 37: 77–86.
23. Cooper AI. Porous materials and supercritical fluids. *Adv Mater* 2003; 15: 1049–1059.
24. Lee ST and Scholz DPK. *Polymeric foams: technology and developments in regulation, process, and products*. Boca Raton: CRC Press, 2008.
25. Bhattacharya S, Gupta RK, Jollands M, et al. Foaming behavior of high-melt strength polypropylene/clay nanocomposites. *Polym Eng Sci* 2009; 49: 2070–2084.
26. Ma W, Ding J and Zhong Q. Foaming of Polystyrene with Supercritical Carbon Dioxide. *Advanced Materials Research* 2013; 669: 366–370.
27. Gendron R, Champagne MF, Tatibouet J, et al. Foaming cyclo-olefin copolymers with carbon dioxide. *Cell Polym* 2009; 28: 1–23.
28. Han X, Koelling KW, Tomasko DL, et al. Continuous microcellular polystyrene foam extrusion with supercritical CO_2. *Polym Eng Sci* 2002; 42: 2094–2106.
29. Han X, Zeng C, Lee LJ, et al. Extrusion of polystyrene nanocomposite foams with supercritical CO_2. *Polym Eng Sci* 2003; 43: 1261–1275.
30. Jiang X-L, Bao J-B, Liu T, et al. Microcellular foaming of polypropylene/clay nanocomposites with supercritical carbon dioxide. *J Cell Plast* 2009; 45: 515–538.
31. Nam PH, Maiti P, Okamoto M, et al. Foam processing and cellular structure of polypropylene/clay nanocomposites. *Polym Eng Sci* 2002; 42: 1907–1918.
32. Otsuka T, Taki K and Ohshima M. Nanocellular foams of PS/PMMA polymer blends. *Macromol Mater Eng* 2008; 293: 78–82.
33. Strauss W and D'Souza NA. Supercritical CO_2 processed polystyrene nanocomposite foams. *J Cell Plast* 2004; 40: 229–241.
34. Xu Z-M, Jiang X-L, Liu T, et al. Foaming of polypropylene with supercritical carbon dioxide. *J Supercrit Fluids* 2007; 41: 299–310.
35. McHugh M and Krukonis V. *Supercritical fluid extraction: principles and practice*. Amsterdam: Elsevier, 2013.
36. Nalawade SP, Picchioni F and Janssen L. Supercritical carbon dioxide as a green solvent for processing polymer melts: processing aspects and applications. *Prog Polym Sci* 2006; 31: 19–43.
37. Yeo S-D and Kiran E. Formation of polymer particles with supercritical fluids: a review. *J Supercrit Fluids* 2005; 34: 287–308.
38. Antunes M, Gedler G and Velasco JI. Multifunctional nanocomposite foams based on polypropylene with carbon nanofillers. *J Cell Plast* 2013; 49: 259–279.
39. Gedler G, Antunes M, Realinho V, et al. Thermal stability of polycarbonate-graphene nanocomposite foams. *Polym Degrad Stabil* 2012; 97: 1297–1304.

40. Gedler G, Antunes M, Realinho V, et al. (eds). *Novel polycarbonate-graphene nanocomposite foams prepared by CO2 dissolution. IOP conference series: materials science and engineering*. Bristol: IOP Publishing, 2012.
41. He T, Liao X, He Y, et al. Novel electric conductive polylactide/carbon nanotubes foams prepared by supercritical CO_2. *Prog Nat Sci Mater Int* 2013; 23: 395–401.
42. Tran MP, Detrembleur C, Alexandre M, et al. The influence of foam morphology of multi-walled carbon nanotubes/poly (methyl methacrylate) nanocomposites on electrical conductivity. *Polymer* 2013; 54: 3261–3270.
43. Shen B, Zhai W, Lu D, et al. Fabrication of microcellular polymer/graphene nanocomposite foams. *Polym Int* 2012; 61: 1693–1702.
44. Wu Y, Wang Z, Liu X, et al. Ultralight graphene foam/conductive polymer composites for exceptional electromagnetic interference shielding. *ACS Appl Mater Interfaces* 2017; 9: 9059–9069.
45. Zhang HB, Yan Q, Zheng WG, et al. Tough graphene−polymer microcellular foams for electromagnetic interference shielding. *ACS Appl Mater Interfaces* 2011; 3: 918–924.
46. Biani A, Dorigato A, Bonani W, et al. Mechanical behaviour of cyclic olefin copolymer/exfoliated graphite nanoplatelets nanocomposites foamed through supercritical carbon dioxide. *Express Polym Lett* 2016; 10: 977–989.
47. Pegoretti A, Dorigato A, Biani A, et al. Cyclic olefin copolymer - silica nanocomposites foams. *J Mater Sci* 2016; 51: 3907–3916.
48. Dorigato A, Pegoretti A and Frache A. Thermal stability of high density polyethylene–fumed silica nanocomposites. *J Therm Anal Calorim* 2012; 109: 863–873.
49. Dorigato A, Pegoretti A, Fambri L, et al. Cycloolefin copolymer/fumed silica nanocomposites. *J Appl Polym Sci* 2011; 119: 3393–3402.
50. Priestley RD, Ellison CJ, Broadbelt LJ, et al. Structural relaxation of polymer glasses at surfaces, interfaces, and in between. *Science* 2005; 309: 456–459.
51. Schadler L, Brinson L and Sawyer W. Polymer nanocomposites: a small part of the story. *Jom* 2007; 59: 53–60.
52. Li YL, Kuan CF, Chen CH, et al. Preparation, thermal stability and electrical properties of PMMA/functionalized graphene oxide nanosheets composites. *Mater Chem Phys* 2012; 134: 677–685.
53. Akın D, Kasgoz A and Durmus A. Quantifying microstructure, electrical and mechanical properties of carbon fiber and expanded graphite filled cyclic olefin copolymer composites. *Compos A Appl Sci Manuf* 2014; 60: 44–51.
54. Dorigato A, Brugnara M and Pegoretti A. Novel polyamide 12 based nanocomposites for industrial applications. *J Polym Res* 2017; 24: 96.
55. Xu XB, Li ZM, Shi L, et al. Ultralight conductive carbon – Nanotube-polymer composite. *Small* 2007; 3: 408–411.